Experimental and Simulation Studies on the Warpage of Coreless Substrate Under Multiple Laminating Process

Zengming Hu[1,2], Guowei Fan[1,2], Jie Xu[1,2], Zeming Fang[1,2], Junqi Tang[3], Li Luo[3], Qianping Rong[3], Qianfa Liu[3], Dashun Liu[4], Dong Lu[5], Ke Xue[5] and Ke Wang[1,2,*]

[1]*Shenzhen Key Laboratory of Intelligent Manufacturing for Continuous Carbon Fiber Reinforced Composites, Southern University of Science and Technology, Shenzhen 518055, China*

[2]*School of System Design and Intelligent Manufacturing, Southern University of Science and Technology, Shenzhen 518055, China*

[3]*Guangdong Shengyi Technology Co., Ltd., Dongguan 523000, China*

[4]*Division of Advanced Engineering Materials, Guangzhou HKUST Fok Ying Tung Research Institute, Guangzhou 511458, China*

[5]*The Hong Kong University of Science and Technology (Guangzhou)*

Abstract: Substrate warpage caused by curing process and thermal cycling is a very important issue in electronic packaging. Considerable efforts have been made to develop methods for predicting, measuring and controlling warpage. The current work focuses on the warpage and stress distribution of coreless substrates during multiple laminating process. Flexural property tests and thermal-mechanical measurements were carried out with samples cured under different lamination cycles in order to investigate the influence of in-plane anisotropic properties on the warpage. The results show that, with the increase of lamination cycles, both flexural modulus and coefficient of thermal expansion (CTE) of the laminates increase. Further, the cure shrinkage of the prepreg during curing, the effects of cure cycles and copper residuals on substrate warpage were examined through finite element analysis. The simulation results show that, after undergoing multiple curing processes, the thermoelastic parameters of the prepreg exhibit a complex relationship with the warpage and stress distribution of the substrate. Due to the increase in the number of material layers, the overall rigidity of the substrate is enhanced, and the average internal stress in the substrate structure decreases. This results in a downward trend in substrate warpage during multiple lamination processes.

Based on the Finite Element Method (FEM) simulation results for the multiple laminating process, some modifications can be made regarding the substrate design and material selection, to optimize fabrication process of coreless substrate.

Keywords: Cure shrinkage, Laminating, Packaging, Prepreg, Substrate, Warpage.

1. INTRODUCTION

In order to adapt to the trend of high integration in electronic products, an important packaging structure—the substrate—is also undergoing miniaturization. One such technical advancement is the development of a new type of substrate known as the coreless substrate. Essentially, a coreless substrate is a type of packaging substrate that has had its core layer removed, leaving only the insulating layers such as resin and prepreg, along with the copper layers. The primary advantage of this design is the significant reduction in substrate volume, with nearly half the space saved in the thickness direction. This greatly optimizes the packaging design space, as illustrated in Figure **1**.

However, coreless substrates are prone to warpage during fabrication or operation due to the absence of support from a rigid core. The increased warpage of the substrate not only leads to defects during manufacturing but also introduces a series of reliability issues during use [1-3], such as inadequate filling, detachment and cracking of solder joints, and solder joint fracture [4, 5].

Consequently, the overall behavior of the prepreg material has a greater impact on the warpage of the coreless substrate. In addition, due to the reduction in thickness, the rigidity of the coreless substrate is also affected, and copper residual in the internal wiring layers will also affect the warpage of the substrate. During the polymerization, because of the cross-linking reaction, prepreg will undergo an increase in density and a corresponding reduction in volume, which is so called cure shrinkage [6]. Cure shrinkage always lead to warpage and residual stress in coreless substrate. There are some works have shown that the contribution of up to 40% of the overall residual deformation due to chemical shrinkage was found in thermosetting composite laminates [7], but many previous works of substrate warpage did not consider the cure shrinkage effect of prepreg [2, 8-10]. Therefore, this study aims to investigate the influence of cure shrinkage on coreless substrate warpage and internal stress by incorporating the shrinkage value of prepreg and the copper residual of wiring layers in both simulation and experimental analysis. The findings of

*Address correspondence to this author at the Shenzhen Key Laboratory of Intelligent Manufacturing for Continuous Carbon Fiber Reinforced Composites, Southern University of Science and Technology, Shenzhen 518055, China; E-mail: wangk7@sustech.edu.cn

E-ISSN: 2311-8717/25

Figure 1: Cored and Coreless substrate [11].

this study are expected to provide valuable insights for the development and design of coreless substrates.

2. MATERIAL PROPERTIES

2.1. Materials

This study employs a method of laminating prepreg samples multiple times to determine the material parameters of the lower prepreg under various lamination conditions. The curing conditions were determined based on the processing guidelines provided by Shengyi Technology Co., Ltd. for the 1078 prepreg. Given the small thickness of a single prepreg, 24 layers of prepreg were stacked during lamination to produce samples with sufficient thickness for bending tests.

Figure **2** outlines the experimental procedure for warpage analysis. Initially, copper-clad laminate (CCL) specimens measuring 40mm×50 mm were prepared. The aspect ratio (Ly/Lx) of the specimens was set to 1.25, in accordance with the dimensions of commercial CCL panels (510mm×405 mm). The type of glass fiber cloth used adhered to the standards of the Institute for Printed Circuits (IPC). The prepreg comprised electronic grade glass fiber cloth with low coefficient of thermal expansion (CTE) and high glass transition temperature (Tg) epoxy resin.

After etching the copper layer on the bottom surface of the copper-clad laminate, sample warpage is observed, resulting from asymmetric residual stresses in the thickness direction (refer to Figure **2**). To prepare copper/core bilayer samples, a passivation film is initially applied to one side of each copper-clad laminate sample before immersing them in the etchant solution. Following the etching process, the bilayer samples are rinsed with tap water and then dried for 2 hours in a convection oven at 105°C to eliminate the influence of moisture absorption on warpage. The warpage of the Cu/laminate bilayer samples is measured using a 4D Scanner three-dimensional scanner (4D Scanner, Cores Inc., Japan), as depicted in Figure **3**. Since a non-contact testing method is employed, the actual warpage profile can be accurately measured.

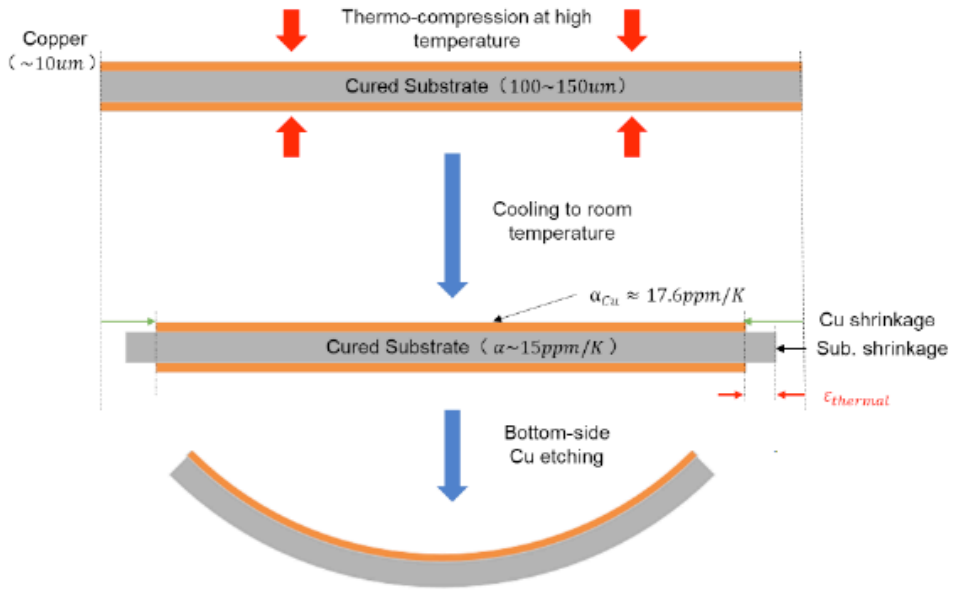

Figure 2: Thermal stress is the cause of warpage in copper/core materials.

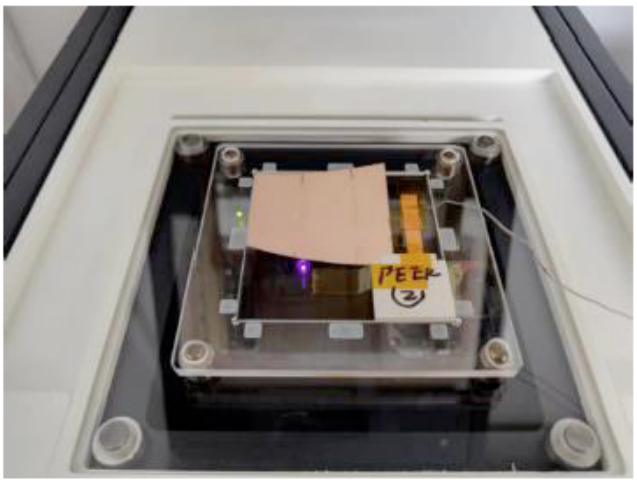

Figure 3: Heating chamber inside the 4D Scanner: Equipped with a camera at the bottom.

To obtain laminate samples with different curing cycles (besides, considering that the prepreg material used in this experiment is too thin (70μm) to conduct bending tests directly), 24 layers of prepreg were stacked during the lamination process to achieve laminate samples with sufficient thickness for bending tests. The lamination and curing conditions were determined in accordance with the processing guidelines provided by Guangdong Shengyi Technology Co., Ltd. for the 1078-type prepreg, as illustrated in Figure **5**.

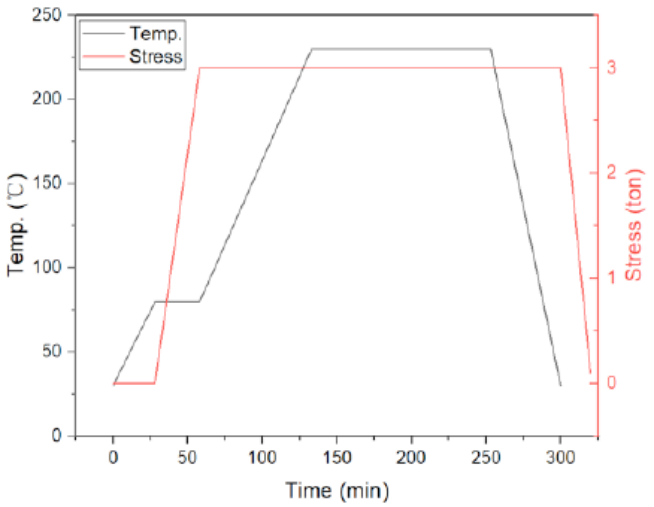

Figure 5: Temperature and stress curve of the laminating process.

2.2. Flexural Properties

To evaluate the elasticity and stiffness of the cured substrate, three-point bending tests were conducted using a small bending fixture to measure the bending modulus of the laminated substrate after curing (refer to Figure **6a**). It is well understood that the epoxy resin layer on the surface of the prepreg significantly contributes to the bending stiffness, leading to the bending modulus of fiber-reinforced epoxy laminates typically being lower than their tensile modulus [12, 13]. Hence, we measured the bending modulus in four

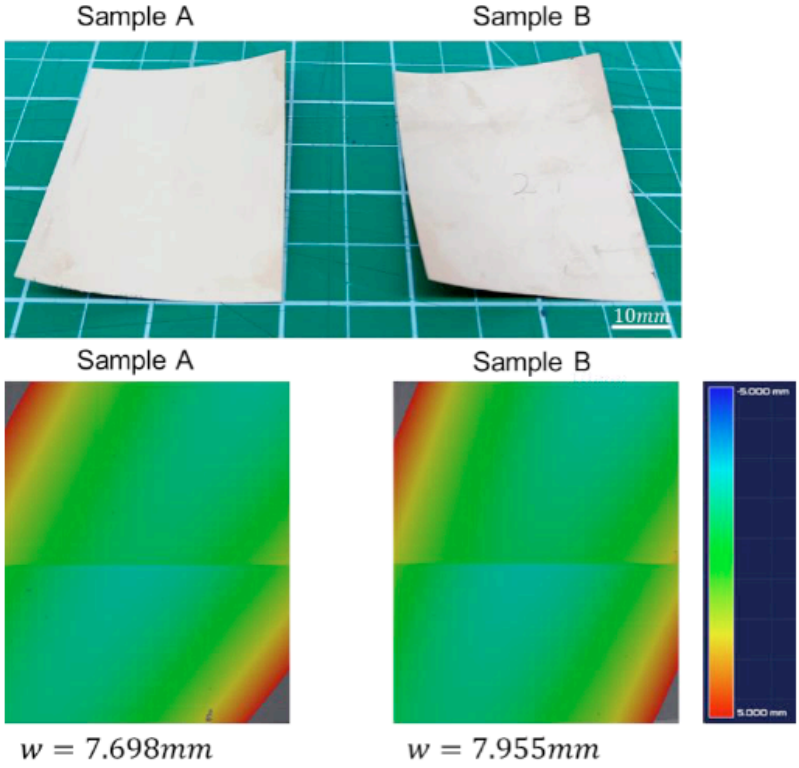

Figure 4: (**a**) Actual warpage of two Cu/substrate bi-material specimens after etching and baking. (**b**) Warpage contour map obtained by use 4D Scanner.

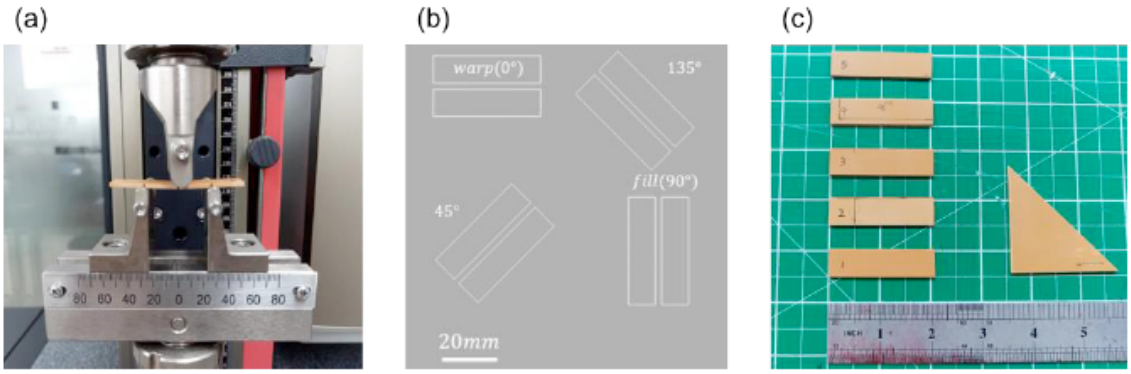

Figure 6: (**a**) Three-point bending test apparatus (**b**) Preparation of samples in four different directions: 0°, 45°, 90° and 135° (**c**) At least 5 samples were prepared in each direction.

directions (0°, 45°, 90°, 135°) for subsequent analysis of the warpage behavior of the copper/laminate bilayer material. Figure **7**(**a**) illustrates the flexural modulus test values of laminate materials in different in-plane directions (0°, 45°, 90°, 135°).

According to ASTM D790, the loading rate of the loading head in the three-point bending test is set at 1 mm/min, and the diameters of the loading head and supports are 6 mm and 1 mm, respectively. Following the lamination process, samples were cut using a high-precision cutting machine to obtain specimens with dimensions of 12.7 mm×54 mm×1.67mm, which were then placed on supports with a span of 27 mm for the bending test. In this study, the bending modulus (*E*) is calculated based on the slope (*m*) of the bending stress-strain curve, with the calculation formula as follows:

$$E_b = \frac{L^3 m}{4bd^3} \quad (1)$$

(E_b - Bending modulus, *L* – Span, *b* - Width of the beam, *d* - Depth of the beam, *m* - Slope of the initial linear segment of the load-displacement curve)

Subsequently, the slope *m* of the linear segment of the load-beam displacement curve obtained from the test is calculated. The slope *m* is obtained in the strain range of [0.05, 0.25]. The calculation formula for bending strain ε_f is as follows:

$$\varepsilon_f = \frac{6Dd}{L^2} \quad (2)$$

(ε_f - Strain on the outer surface, *D* - Maximum displacement at the center of the beam, *L* – Span, *d* - Depth of the beam) Figure **8**(**a**) illustrates the flexural modulus test values of laminate materials under different curing cycles. As depicted in Figure **8**(**a**), with an increase in the number of curing cycles, there is a slight increase in the flexural modulus of laminate materials. This is attributed to the presence of a small portion of resin remaining uncured in the previous curing cycle, which subsequently cures during the subsequent lamination process, leading to an enhancement in the material modulus.

The flexural modulus was measured by using universal machine (Zwick Z005, ZwickRoell, Germany).

2.3. Coefficients of Thermal Expansion

Due to one of the primary causes of residual stress being the differences in CTE between different materials, accurately measuring the in-plane CTE of

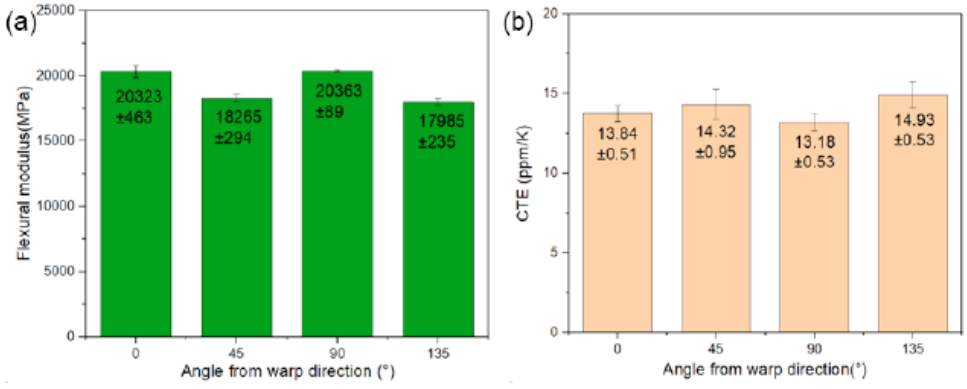

Figure 7: (**a**) Flexural modulus of the substrate in different in-plane directions (0°, 45°, 90°, 135°). (**b**) CTE of the substrate in different in-plane directions (0°, 45°, 90°, 135°).

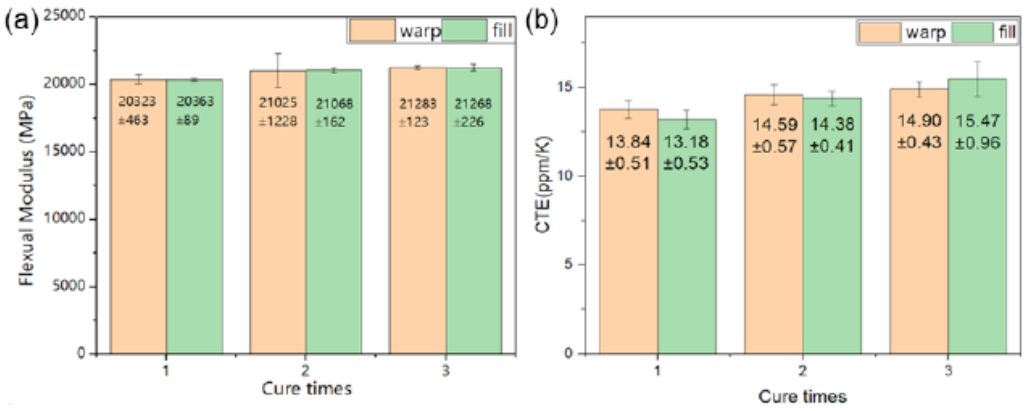

Figure 8: (**a**) Flexural modulus of the substrate in different cure times (1, 2, 3). (**b**) CTE of the substrate in different cure times (1, 2, 3).

the substrate is of significant importance for simulation accuracy.

According to TM650 2.4.24.5, the specimens with sizes of 12mm×2mm×0.075mm were cut on the substrate in four directions within the plane (0°, 45°, 90°, 135°) to measure its linear CTE (Figure **7**(**b**)). These samples were then placed in the chamber of a Thermomechanical Analysis (TMA) device. Thermal strain was measured from room temperature (25°C) to 300°C at a heating rate of 5 ℃/min. The slope of the obtained dL/dL_0-temperature curve represents the thermal expansion coefficient of the sample. The test results are shown in Figure **7**(**b**).

To investigate the influence of curing cycles on the performance of laminates, the variations in CTE of laminate materials under different curing cycles were also measured. Figure **8**(**b**) illustrates the trends of CTE changes in the warp and fill directions of laminate materials at different curing cycles. With an increase in the number of curing cycles, there is a slight increase in CTE in both directions.

The CTE was measured by using TMA (TMA402F3 Hyperion, NETZSCH, Germany).

2.4. Cure Shrinkage

Two types of shrinkage occur in a thermosetting resin during the thermal cure cycle. The first is related to the reduction in volume as a result of crosslinking, and it is denoted as chemical shrinkage. This type of shrinkage solely depends on the progression of the degree of cure in the resin. The second type of shrinkage occurs as a result of heating or cooling due to thermal deformation and it is characterized by CTE.

Figure **9** shows the procedure used to model the cure shrinkage of the substrate. The cure shrinkage strain was implemented in the FEM program as a fit value as follows: First, a guess value (ε_{cure_guess}) of the cure strain was assigned to the model. Then the cooling process from the cure temperature (230°C) to the room temperature (25°C) was added. Finally, if the predicted warpage curve did not fit to the experimental one, the value of the $\varepsilon_{cure_guess}$was changed so that the predicted warpage curve fits the experimental one.

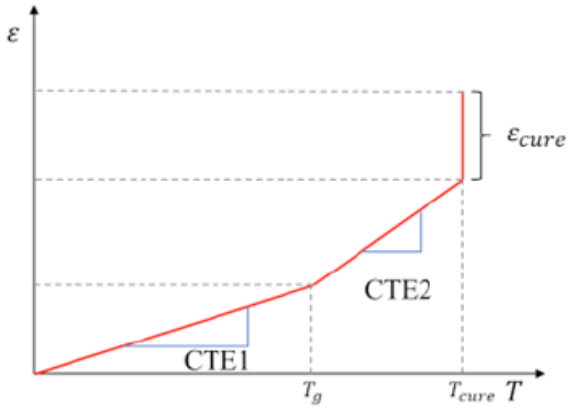

Figure 9: Material model for the determination of the cure strain.

The in-plane shear modulus *G* is calculated from the bending modulus in the longitudinal direction (θ=0°) and diagonal direction (θ=45°) using the following formula [14].

$$\frac{1}{E_x} = \frac{1}{E_L}\cos^4\theta + \frac{1}{E_T}\sin^4\theta + \left(\frac{1}{G_{LT}} - \frac{2\nu_{LT}}{E_L}\right)\sin^2\theta\cos^2\theta \quad (3)$$

$$\frac{1}{E_y} = \frac{1}{E_L}\sin^4\theta + \frac{1}{E_T}\cos^4\theta + \left(\frac{1}{G_{LT}} - \frac{2\nu_{LT}}{E_L}\right)\sin^2\theta\cos^2\theta \quad (4)$$

The subscripts *L* and *T* represent the two principal material directions (longitudinal and transverse), while x and y denote two orthogonal directions rotated counterclockwise by an angle θ from the principal directions. Here, ν_{LT} is the Poisson's ratio in the two-dimensional material direction. Since the 1078-type glass fiber woven fabric has the same number of yarns in the longitudinal and transverse directions, we can consider the substrate as a

balanced isotropic composite material. For balanced isotropic composite materials, it can be approximately assumed that $E_L \approx E_T$.

Combining equation (3), (4), the principal shear modulus is obtained as follows:

$$G_{LT} = \frac{1}{\frac{4}{E_{45^\circ}} - \left[(1-2v_{LT})\frac{1}{E_L} + \frac{1}{E_T}\right]} \quad (5)$$

From the measured directional CTEs, thermal deformation of the laminate under temperature variation ΔT can be well described using a 2-D thermal strain tensor with CTE values of α_{11}, α_{22} and α_{12}, where 1 and 2 indicate warp and fill directions of laminates, respectively ($\alpha_{11} = \alpha_{0^\circ}$ and $\alpha_{22} = \alpha_{90^\circ}$). While the thermal strain of an ideally balanced orthotropic laminate is described by Eq. (6), it is judged that the actual laminates in this study behave with a strain set of Eq. (7) where the non-zero shear strain exists.

$$\varepsilon^T_{orthotropic} = \begin{pmatrix} \varepsilon^T_1 \\ \varepsilon^T_2 \\ 0 \end{pmatrix} = \begin{pmatrix} \alpha_{11} \\ \alpha_{22} \\ 0 \end{pmatrix} \Delta T \quad (6)$$

$$\varepsilon^T_{anisotropic} = \begin{pmatrix} \varepsilon^T_{11} \\ \varepsilon^T_{22} \\ \varepsilon^T_{12} \end{pmatrix} = \begin{pmatrix} \alpha_{11} \\ \alpha_{22} \\ \alpha_{12} \end{pmatrix} \Delta T \quad (7)$$

The shear CTE α_{12} can be calculated from the measurements of α_{45° and $\alpha_{135^\circ}$by the following strain tensor transformation (Eq. (8) and Eq. (9))

$$\alpha_x = \alpha_{11}\cos^2\theta + \alpha_{22}\sin^2\theta + 2\sin\theta\cos\theta\alpha_{12} \quad (8)$$

$$\alpha_y = \alpha_{11}\sin^2\theta + \alpha_{22}\cos^2\theta - 2\sin\theta\cos\theta\alpha_{12} \quad (9)$$

When $\theta = 45^\circ$,we have:

$$\alpha_{45^\circ} = \frac{1}{2}\alpha_{11} + \frac{1}{2}\alpha_{22} + \alpha_{12} \quad (10)$$

$$\alpha_{135^\circ} = \frac{1}{2}\alpha_{11} + \frac{1}{2}\alpha_{22} - \alpha_{12} \quad (11)$$

Subtracting the Eqs. (10), (11), the α_{12} is simply calculated as follows:

$$\alpha_{12} = \frac{1}{2}(\alpha_{45^\circ} - \alpha_{135^\circ}) \quad (12)$$

According to Eq. (12), the calculated shear CTE α_{12} is 0.35 ppm/K for substrate.

The modulus and CTE data referenced above are both derived from the results presented in Section 2.3.

2.5. The Resolution of Cure Shrinkage

In general, when the width-to-thickness ratio of the studied object exceeds 10, it is considered appropriate to employ shell elements for simulation. Given the large width-to-thickness ratio of the copper/substrate bi-material, the system can be simplified into a two-dimensional plane problem for analysis.

The simulation for determining the cure shrinkage-induced warpage was conducted on actual-sized samples measuring 40 mm × 50 mm by using ABAQUS (Abaqus2021, Dassault, France). The samples were modeled using composite shell elements (S4R), with a mesh consisting of 8000 elements. It was assumed that the thermal curing of the epoxy resin matrix was completed at the highest temperature, and then residual stress was generated due to the prepreg cure shrinkage and the mismatch in CTE between the prepreg and the copper foil. The isotropic modulus of the seed copper foil was 120 GPa, with a Poisson's ratio of 0.345 and a CTE of 17.8 ppm/K. The static, general procedure incorporating geometric nonlinearity was used for the simulation module.

By comparing the actual warpage values of the copper/laminate samples measured using 4D Scanner at 25°C, during the cooling process in finite element simulation, an approach incorporating the equivalent of curing shrinkage (within the range of 230°C to 229°C) was introduced to simulate the room temperature warpage results of the copper/laminate samples. After iteratively adjusting the curing shrinkage values, the final equivalent curing shrinkage of the 1078 prepreg was determined to be 750 ppm/K, as depicted in the warpage contour map shown in Figure **10**.

3. WARPAGE SIMULATION

3.1. Analysis of Warpage Mechanism

The fundamental reason for warpage in coreless substrates is the internal stress of the board exceeding the structural strength of the board. The main causes are as follows:

(1) Compared to build-up substrates, coreless substrates lack rigidity due to the absence of a core.

(2) The mismatch in CTE and modulus between the laminate inside the substrate and the copper layer results in thermal stress during cooling, ultimately converting into residual stress stored within the structure.

(3) The cure shrinkage effect caused by molecular cross-linking during the lamination process of prepreg also contributes to residual stress.

Under the coupling of these factors, the overall structure tends to warp upwards or downwards.

Considering the complexity of copper circuit patterns, modeling them one-to-one would be extremely laborious and intricate. Moreover, it would

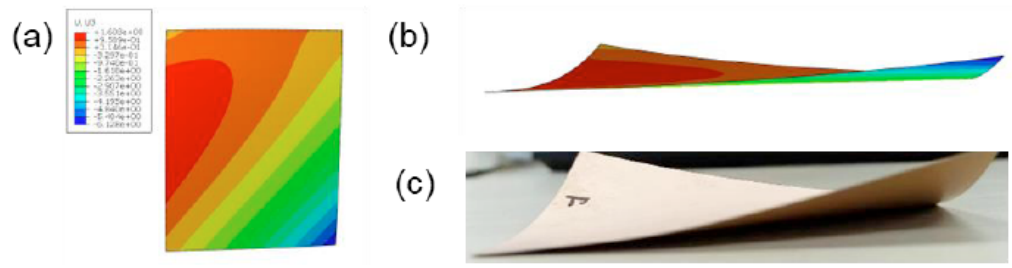

Figure 10: (**a**) Simulation results of room temperature warpage for copper/substrate (**b**) Side view (**c**) Photograph of copper/substrate samples at room temperature.

lead to increased demands on subsequent mesh partitioning and computational burden. Therefore, adopting a rational design to simplify the modeling of wiring layers becomes particularly important.

Due to the solder mask (SM) layer on top of the copper circuit layer filling the gaps in the copper circuit pattern, the wire layer essentially becomes a composite material composed of green oil and copper interleaving. We can obtain this according to the rules of mixture (ROM) for composite materials:

$$E_{11} = E_f V_f + E_m V_m \tag{13}$$

$$E_{22} = \frac{E_f E_m}{E_f V_m + E_m V_f} \tag{14}$$

$$v_{12} = v_m V_m + v_f V_f \tag{15}$$

$$v_{21} = \frac{E_{22}}{E_{11}} v_{12} \tag{16}$$

$$\alpha_{11} = \frac{\alpha_f E_f V_f + \alpha_m E_m V_m}{E_f V_f + E_m V_m} \tag{17}$$

$$\alpha_{22} = (1 + v_f)\alpha_f V_f + (1 + v_m)\alpha_m V_m - \alpha_{11} v_{12} \tag{18}$$

(*E*: Young's modulus, α: Coefficient of thermal expansion, *V*: Volume fraction, *v*: Poisson's ratio, *f, m* - Represent Cu and solder mask respectively.)

The volume fraction refers to the respective volumes occupied by the solder mask and copper pattern layers within the composite material layer.

Taking into account the influence of temperature and time on stress during the molding process, prepreg select a temperature-dependent linear elastic model. The specific material parameters are shown in Table **1**. The material parameters of the solder mask (AUS308) were obtained from the official website of Taiyo Ink. The pattern of the copper circuit determines the size of the final copper residue rate. In our simulations, we found that the copper residue rate has impact on the warpage of coreless substrates.

The model for the bare board process mainly consists of copper layers, base insulation material - prepreg, and solder mask layer. Although copper's thermo-mechanical properties show no significant change with temperature variations, the solder mask layer experiences substantial changes in modulus and CTE around T_g. Therefore, the material parameters of the equivalent layer (Cu + SM) obtained from the rule of mixtures will consider the T_g of the solder mask layer and be set as temperature-dependent linear elastic materials. The material parameters refer to Table **2**. As shown in Figure **11**, the finite element model used in

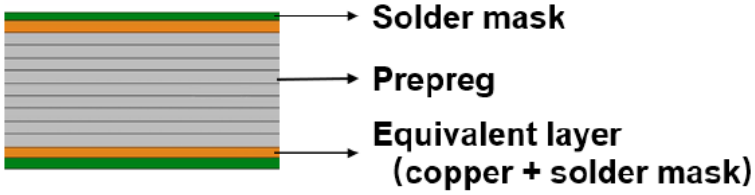

Figure 11: Schematic of simplified finite element model for bare board.

Table 1: Material Properties

Material	CTE (1/°C)	Modulus (GPa)	Poisson' Ratio
Solder mask	60e-6(<100°C) 130e-6	4.1(30°C) 0.35(260°C)	0.35
Copper	17.6e-6	132	0.33

this paper mainly consists of the core layers (two copper layers plus one layer of prepreg) and the solder mask layer.

Table 2: Thickness of Each Layer

Material	Thickness (μm)
Solder mask(top)	10
Wire layer(top)	13
Prepreg	130
Wire layer(bottom)	13
Solder mask(bottom)	12

3.2. Boundary Condition

The curing temperature for the green solder mask is 150°C, therefore, the conditions for simulating the green solder mask curing process are set to 150°C - 30°C. The boundary conditions are shown in Figure **12**. Additionally, heat transfer processes during cooling are neglected, assuming that the overall temperature of the device is instantly equal to the ambient temperature. The temperature field is applied to all nodes, while it is assumed that the zero-stress temperature for all devices is 150°C, indicating that the overall structure is in a zero-stress state at the initial moment.

The mesh division for the bare board warpage adopts C3D8R elements, with a global approximate size of 1mm used for modeling. Each layer is divided into 19,500 elements, resulting in a total of 305,000 elements globally. Since a quarter model was used for modeling, Figure **12** displays the overall model's boundary conditions in the x, y, and z directions. In the quarter model, to restrain rigid body displacement, two symmetric surfaces are set as symmetric constraints, and a point is chosen to constrain the displacement in the intersecting edge direction of the two symmetric surfaces on one of the symmetric surfaces.

3.3. Discussion

The magnitude of warpage deformation in coreless substrates is significantly influenced by factors such as the level of CTE matching between different layers, the residual copper content in the wiring layers, and the cure shrinkage effect of the resin. The residual copper rate, which refers to the percentage of residual copper in non-designated regions after the etching process, can affect the internal stress distribution and warpage. Currently, the prevailing recommendation for reducing warpage deformation involves using materials with similar CTE to construct the substrate, thereby mitigating significant warpage deformation. This study primarily investigates the effects of prepreg cure shrinkage and residual copper content in the copper layer on the magnitude of warpage deformation in the bare board process.

In the aforementioned simulations, the green solder mask curing process was simulated with and without considering cure shrinkage. The results, depicted in Figure **13**, demonstrate that the introduction of cure shrinkage leads to a decrease in warpage value by approximately 0.23mm compared to the scenario where cure shrinkage is not considered. From the result of Figure **13**, we can confirm that the cure shrinkage of prepreg during the curing process shows a significant effect on warpage simulation. The decrease in warpage might be attributed to the cure shrinkage improving the elastic modulus of the prepreg, which led to a reduced mismatch between the prepreg and the circuit layer. Therefore, it is essential to consider the cure shrinkage of the prepreg in subsequent simulations.

Based on the model incorporating cure shrinkage, another study was conducted to investigate the effect of the residual copper rate in the wiring layers on bare board warpage. The influence of simultaneous changes in the residual copper rate in the upper and

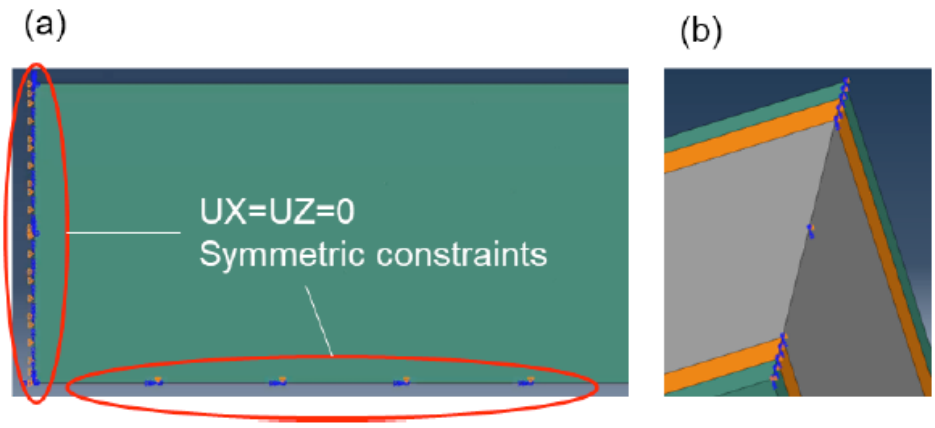

Figure 12: (**a**) Symmetric constraints in the x and z directions of the model. (**b**) Geometric constraints in the y (thickness) direction of the model.

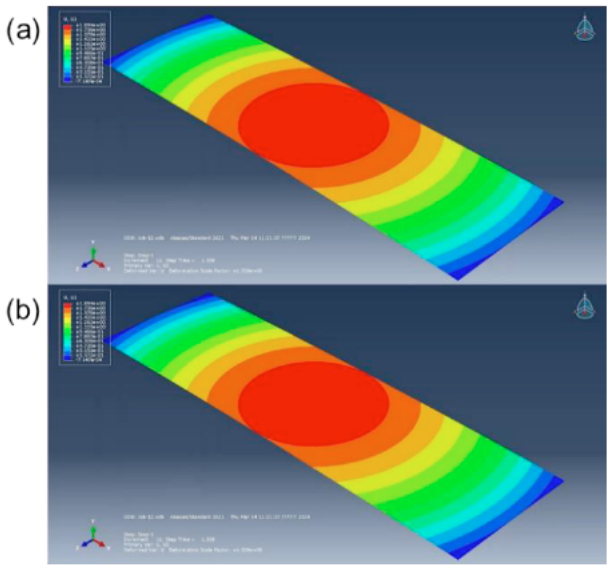

Figure 13: Comparison of bare board warpage values: (**a**) Without including cure shrinkage: 2.085mm; (**b**) Including cure shrinkage: 1.849mm.

lower wiring layers on bare board warpage is illustrated in Figure **13**. According to the simulation result, it can be concluded that, without altering the thickness of the wiring layers, appropriately increasing the residual copper rate can effectively reduce warpage. Furthermore, it is essential to ensure that the copper patterns on both sides are as consistent as possible.

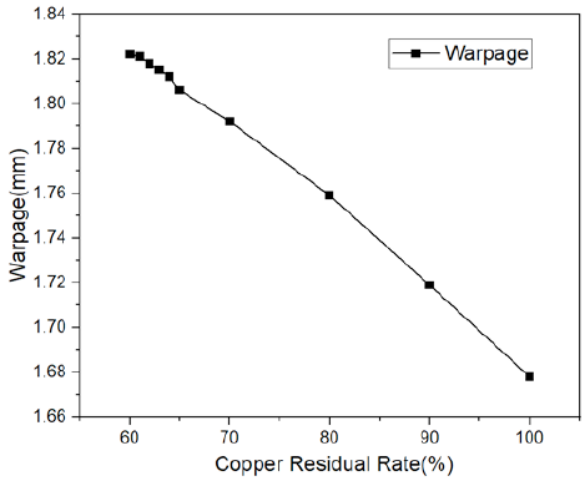

Figure 14: Influence of residual copper rate in wiring layers on bare board warpage.

4. EFFECTS OF MULTIPLE LAMINATING PROCESS

Figure **15** illustrates the process of multiple laminating and solder mask curing in simulation. During the finite element analysis, it is assumed that material properties change during the manufacturing process. The temperature condition of simulation for the laminating cooling process is from 230°C to 30°C. Considering the substrate's symmetry, to save computational time, the finite element analysis will use a 1/4 model for modeling and calculation. The material parameters of the laminate at various curing cycles are sourced from the experimental data presented in Section 2.

4.1. Results

Figure **16** shows the analysis results for the stress distributions and warpage that occurred in the substrate cooling back to room temperature after the first laminating process and the removal of the press compression for laminating. In actual cooling process from 230°C to 30°C after 1st laminating process, the different thermal strain would be generated in the copper and cured prepreg due to the difference in CTE and modulus. Besides, after cooling process, the thermal strain mismatch between the circuit layer and prepreg were generated since the CTE and modulus of circuit layer are higher than prepreg. These led to the internal stress and warpage. The simulation results following the initial lamination indicate a warpage of approximately 8.4 μm in the substrate, and the internal stress was approximately 28.5 MPa.

After the second laminating process and the removal of the press compression for laminating. Internal stress occurred in substrate was approximately 32.9MPa, and the warpage was approximately 3.74μm.

After third laminating, internal stress in substrate was increased to 34.67MPa, while the warpage decreased to 2.05μm. These results indicate that, although multiple laminating steps slightly reduce substrate warpage, the overall improvement is limited, and internal stress continues to accumulate within the substrate.

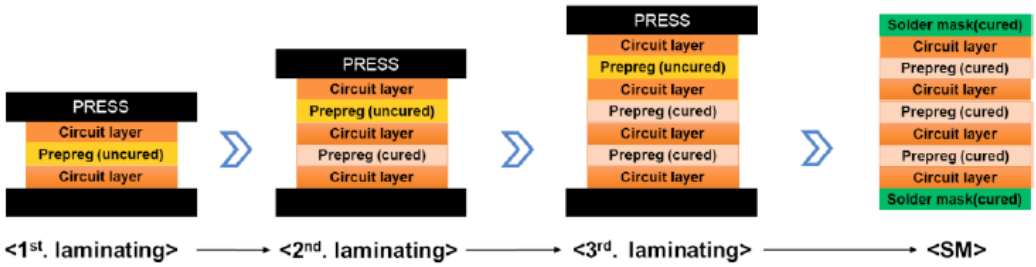

Figure 15: Schematic of Multiple Laminating Process and Solder Mask Laminating Process in simulation.

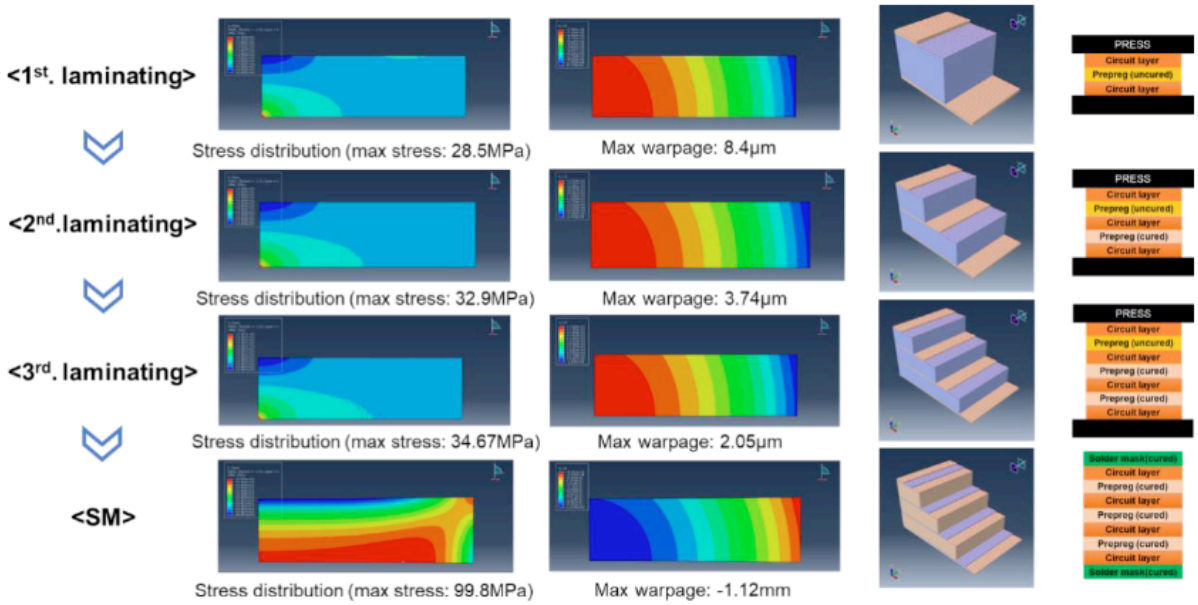

Figure 16: Analysis results of the substrate after 1st., 2nd., 3rd. and solder mask laminating.

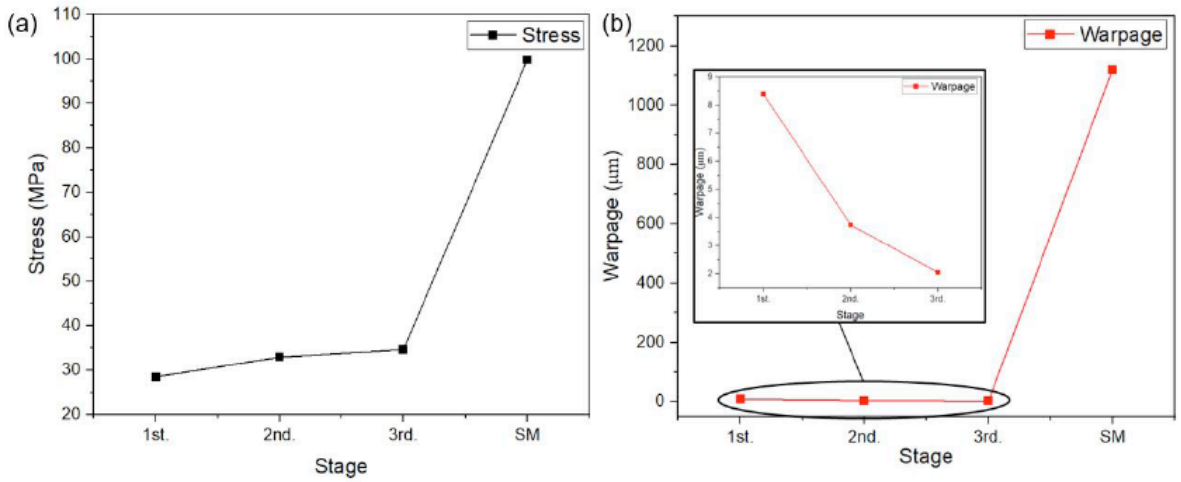

Figure 17: Max stress and warpage (absolute value) in different stages.

The warpage and stress distributions in the substrate were evaluated after the solder mask laminating process was completed and the system had naturally cooled to room temperature. Because of the high coefficient of thermal expansion (CTE) of the solder mask, the warpage of the substrate rapidly increases to 1.12mm due to the deformation caused by solder mask curing. Besides, the internal stress accumulated within the substrate significantly increases to 99.8MPa during the solder mask curing process.

The results from Figures **17** indicate that during the 1st., 2nd. And 3rd. laminating process of prepreg in multiple laminating process of substrate, warpage generated are very low. However, the internal stress continuously accumulates within substrate. This phenomenon can be attributed to the increasing modulus of the prepreg with additional curing cycles.

Regarding warpage, the increasing times of laminating process enhances the overall rigidity of the substrate due to the increased number of layers and the development of a symmetrical structure in the thickness direction. This increased rigidity suppresses warpage, resulting in minimal warpage values during this stage, with a trend towards further reduction. Adding more layers can make the substrate structure more uniform and symmetric, which helps reduce warpage caused by uneven thermal expansion. Besides, more layers can help distribute thermal stress more evenly, reducing local stress concentrations and thus decreasing the degree of warpage. And higher overall rigidity results in less deformation of the

substrate under the same stress, directly reducing warpage.

In SM cure stage, significant differences in the coefficient of thermal expansion and modulus between the solder mask, wiring layers, and prepreg layers, combined with varying thicknesses of solder mask on the top and bottom surfaces of the substrate, result in substantial warpage and an increase in internal stress after the solder mask curing process. Therefore, in the design of the substrate, in addition to considering the differences in the coefficients of thermal expansion between different material layers, maintaining symmetry in thickness is also crucial for reducing the final warpage of the substrate.

For internal stress, although the simulation results show that as the lamination process progresses, warpage gradually decreases while internal stress gradually accumulates, the number of material layers in the substrate also gradually increases with the number of laminations. (15) Considering the average internal stress in the structure, the average internal stress in each layer should be gradually decreasing, as indicated by Eq. (19).

$$\bar{\sigma}_{total} = \frac{1}{H}\sum_i h_i \bar{\sigma}_i \quad (19)$$

(H: total thickness of the structure h_i: thickness of each layer, $\bar{\sigma}_i$: average internal stress of each layer)

Thus, it's necessary to address the warpage and internal stress that arise during the multiple laminating processes. Specifically, developing strategies to mitigate both warpage and internal stress is vital for minimizing the final warpage of the substrate.

CONCLUSION

The current study proposes an approximate solution method for the warpage and stress distribution of coreless substrates during the continuous lamination process, utilizing the finite element software Abaqus for simulation and analysis. It also considers the impact of the cure shrinkage effect of prepreg on warpage during this process. The research indicates that the in-plane anisotropy of the thermoelastic parameters of the prepreg is a significant cause of the diagonal warpage observed in copper-prepreg bi-materials. Furthermore, the results of the finite element analysis show that the cure shrinkage effect of the prepreg can appropriately reduce warpage during the manufacturing process of coreless substrates.

The study further indicates that, with the increase in the number of lamination cycles, the flexural modulus of the prepreg shows a slight increase. Additionally, due to the increase in the number of material layers in the substrate, the overall rigidity of the substrate is enhanced, and the average internal stress in the substrate structure decreases. This results in a downward trend in substrate warpage during multiple lamination processes.

Based on the FEM simulation results for the multiple laminating processes, some modifications can be made regarding the substrate design and material selection, to optimize fabrication process of coreless substrate.

REFERENCES

[1] Cho, S. and S. Lee, Study on Behavior Characteristics of Embedded PCB for FCCSP Using Numerical Analysis. Journal of the Microelectronics and Packaging Society, 2020. 27(1): p. 67-73.

[2] Straubinger, D., *et al.,* Modelling of temperature distribution along PCB thickness in different substrates during reflow. Circuit World, 2020. 46(2): p. 85-92. https://doi.org/10.1108/CW-07-2019-0074

[3] Su, S. and M. Jian, Effects of surface finish on the shear fatigue of SAC-based solder alloys. IEEE Transactions on Components, Packaging and Manufacturing Technology, 2019. 10(3): p. 457-466. https://doi.org/10.1109/TCPMT.2019.2942806

[4] Sung, R., K. Chiang, Y.P. Wang, and C. Hsiao. Comparative analysis of electrical performance on coreless and standard flip-chip substrate. in 2007 Proceedings 57th Electronic Components and Technology Conference. 2007. IEEE. https://doi.org/10.1109/ECTC.2007.374062

[5] Masazumi, A., Characterization of chip scale package materials. Microelectron. Reliab, 1999. 39: p. 1365. https://doi.org/10.1016/S0026-2714(99)00059-1

[6] Kravchenko, O.G., *et al.,* Prediction of the chemical and thermal shrinkage in a thermoset polymer. Composites Part A: Applied Science and Manufacturing, 2014. 66: p. 35-43. https://doi.org/10.1016/j.compositesa.2014.07.002

[7] Kravchenko, O.G., S.G. Kravchenko, and R.B. Pipes, Cure history dependence of residual deformation in a thermosetting laminate. Composites Part A: Applied Science and Manufacturing, 2017. 99: p. 186-197. https://doi.org/10.1016/j.compositesa.2017.04.006

[8] Kim, J., et al., Warpage issues and assembly challenges using coreless package substrate. IPC APEX EXPO 2012, 2012. 3: p. 2023-2047.

[9] Kurashina, M., *et al.,* Low Warpage Coreless Substrate for IC Packages. Transactions of The Japan Institute of Electronics Packaging, 2012. 5: p. 55-62. https://doi.org/10.5104/jiepeng.5.55

[10] Tatikola, R., M. Chowdhury, R. Chen, and Z. Jin. Simulation study of power delivery performance on flip-chip substrate technologies. in 2004 Proceedings. 54th Electronic Components and Technology Conference (IEEE Cat. No.04CH37546). 2004.

[11] Samsung Electro-Mechanics Corp. "Coreless RF-SiP". Available from: https://www.samsungsem.com/cn/product/substrate/package-substrate.do.

[12] Lee, T.I., C. Kim, M.S. Kim, and T.S. Kim, Flexural and tensile moduli of flexible FR4 substrates. Polymer Testing, 2016. 53: p. 70-76. https://doi.org/10.1016/j.polymertesting.2016.05.012

[13] Zweben, C., W. Smith, and M.D. Wardle. Test Methods for Fiber Tensile Strength, Composite Flexural Modulus, and Properties of Fabric-Reinforced Laminates. 1979.

[14] Agarwal, B., L. Broutman, B. Agarwal, and L. Broutman, Analysis and performance of fiber composites Second edition. 1990: John Wiley & Sons.

[15] Kim, J.S., Paik, K.W., Kim, B.K. *et al*. The finite element analysis of internal stresses during sequential build-up of lamination-based thick-film multilayer substrates. Journal of Materials Science: Materials in Electronics 11, 45-56 (2000). https://doi.org/10.1023/A:1008956204189

Received on 20-05-2025 Accepted on 15-06-2025 Published on 18-06-2025

https://doi.org/10.12974/2311-8717.2025.13.01